AN ACCURATE PATH PLANNING ALGORITHM BASED ON TRIANGULAR MESHES IN ROBOTIC FIBRE PLACEMENT

Lina Li,* Xingang Wang,* De Xu,* and Min Tan**

Abstract

Based on triangular meshes, an accurate path planning algorithm with the commonly used four laying angles in the robotic fibre placement (RFP) is proposed. The initial paths with different laying angles are firstly produced. Along certain directions, the offset curves are then obtained by a method of variable offset distances which are affected by the placement error and the number of fibre tows. The simulation results verify the effectiveness of this method.

Key Words

Robotic fibre placement, path planning, triangular meshes, offset curves

1. Introduction

Fibre reinforced composites have many advantages over traditional structure materials such as high strength-to-weight ratio, high stiffness-to-weight ratio, resistance to corrosion and versatility in meeting design requirement which make them widely used in aerospace and automotive industries [1]–[2]. Automated placement technology with labour-saving and low-cost characteristics is developed for the manufacturing of composite structures. It includes automated tape placement (ATP) and robotic fibre placement (RFP) which are both advanced manufacturing technologies. With a certain width of the composite tape, one of the most important shortcomings of ATP is its limitation on acceptable mould shape and lay-up paths. For most surfaces, ATP may lead to gaps between tapes if no overlap is used, or result in an uneven surface if lots of overlaps are adopted. However, RFP utilizes a placement head to simultaneously lay down a large number (up to 32) of the impregnated fibre tows, then the fibre tows are placed by an elastomeric roller side by side and compacted on the mould surface. It is capable of cutting and restarting each fibre tow separately to achieve all desired orientations and fabricate complex structures with curvature changing significantly [3]–[4].

Path planning is involved in many applications, and there are lots of the methods to plan the desired paths [5]–[6]. Meanwhile, path planning is also one of the key technologies in RFP and it determines the distribution way of the fibre tows placed on the mould surface. The results of the path planning directly determine the precision of the component forming and the efficiency of the placement. The methods of path planning have been widely studied by the researchers and some achievements have been acquired in this field. A novel path planning algorithm called the surface curve algorithm for RFP is proposed in [7]. This method is based on the parametric equation of the mould surface. The initial reference path is computed by the surface-plane intersection strategy and the next path is offset from the initial path along the surface by a distance with maximal tow-width in a perpendicular direction. Subsequent offset paths continue to be formulated until the mould surface is completely covered. A method with varied offset distance is developed to guarantee all the fibre tows to be placed on the mould surface completely in [8]. In their work, the differential geometry is used to ensure that the adjacent paths meet the requirement of the specified small gaps and overlaps in order to improve the composite quality. The determination of the roller location which allows a smooth roller motion along the generated path is also taken into account. In [9], based on the mathematical model of the general revolved structures, an analytical algorithm about the path planning is deduced. In [10], a new parallel equidistant path generation algorithm using the geodesic line is introduced. This algorithm requires the distance between the adjacent paths equally along the geodesic direction. The majority of algorithms introduced above are mainly carried out on the mould expressed by parameter equation or mathematical expression. However, in most industries, the parametric equations of most composite structures are not available.

The three-dimensional measurement and the reverse modelling are rapidly developed in a variety of applications [11]. The meshed surface has recently become

* Research Center of Precision Sensing and Control, Institute of Automation, Chinese Academy of Sciences, China; e-mail: {lilina2013, xingang.wang, de.xu}@ia.ac.cn

** The State Key Laboratory of Management and Control for Complex Systems, Institute of Automation, Chinese Academy of Sciences, China; e-mail: min.tan@ia.ac.cn

the focus of interest and has been used in the industrial fields of aerospace, automobile and shipbuilding which are closely related to the manufacturing industry, because its geometric computation is simpler and more robust than that of the parametric surface [12]. In [13,] a path planning algorithm based on meshed surfaces with fixed angles which are commonly used in RFP is stated. But there would be many times of cutting and restarting the fibre tows during one path placing, which inevitably causes the gaps or overlaps between fibre paths and also reduces the efficiency of placement. In [14], a path planning algorithm for the open-contoured surface with isometric laying is presented. The surface can be completely covered with this method. But during the offsetting process, the equidistant width of fibre tows on the complex surface might not be placed completely. In [15], based on meshed triangles, the algorithm with the fixed angles and the arc divided equally is produced. The method uses the universal rotation transformation to ensure the placement angle is invariant. But the number of the fibre tows between paths is varied which needs the placement head to cut and restart fibre tows frequently and it does not consider the placement error which could make the fibre tows to be pressed on the mould surface totally.

The motivation of this work is to develop a path planning algorithm based on triangular meshes for RFP in which fibre tows can be placed on the mould surface completely, and there are minimal gaps and overlaps between adjacent courses which are constituted by a number of fibre tows.

The rest of the paper is organized as follows: the overall methodology of RFP path planning is described in Section 2; The algorithm preliminary is presented in Section 3; Section 4 illustrates the accurate path planning method, including initial paths generation and offset paths construction, the offset distance and the number of fibre tows determination; The simulation results are given in Section 5; The paper's conclusion is provided in Section 6.

2. Overall Methodology of Path Planning in Robotic Fibre Placement

2.1 The Robotic Fibre Placement Process

The typical configuration of RFP is shown in Fig. 1, which mainly includes a robot manipulator, a placement head and a mould surface. The placement head is used for the tows to provide all desired orientations and three-dimensional locations. A compaction roller which is mounted on the end of the placement head is applied to remove trapped air or void between tows and the substrate material. So the fibre tows are bonded together. By adopting a robotic manipulator and multiple fibre tows, RFP could make the composite structures with rapid manufacturing and mass production, and it can cut, start and feed each fibre tow separately to control the laying width, which makes it suitable for the fabrication of complex structures.

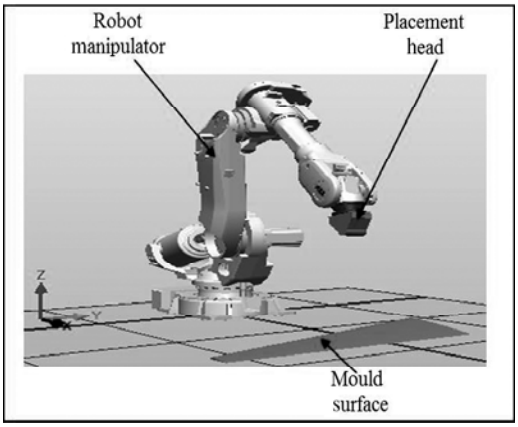

Figure 1. Configuration of RFP.

2.2 The Path Planning Algorithm

The proposed algorithm in this paper is based on meshed triangles and uses the Stereo Lithography (STL) file format to express the mould surface. Firstly, the topology reconstruction of meshed triangles should be conducted. The assumed basis for path planning in RFP is that given an initial path, the next path is offset along the surface at a distance in a perpendicular direction from the given path [7]. In order to meet the requirement, there must be a given path, which is also called the initial path. So the initial path is then produced using the rotation transformation, considering the variation of the triangle's normal vector. The next path is obtained by the varied offset distance method along the offset direction. Each offset distance is determined by the placement error and the number of the fibre tows. Based on the method above, the overall strategy of path planning is shown in Fig. 2.

During the RFP, the basic constitution is the fibre tow, which produces strength and the stiffness along its length when it is cured with heat and pressure. The placement head can deal with 32 adjacent fibre tows in one course, and multiple courses are placed alongside each other to form a ply, and multiple plies are placed atop one another to form the desired structure.

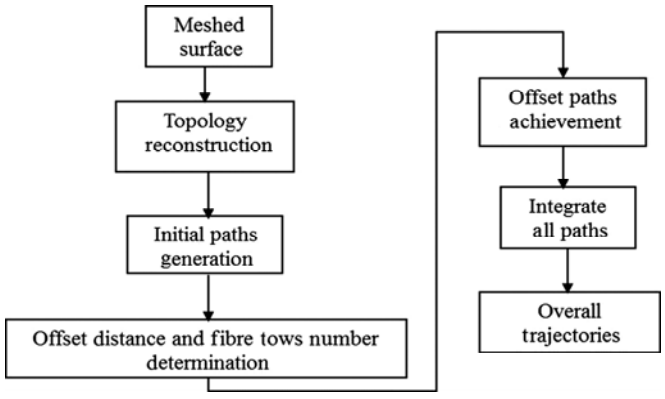

Figure 2. Overall strategy for RFP path planning algorithm.

3. Algorithm Preliminary

3.1 Topology Reconstruction of Triangular Meshes

The STL model which is a type of data files is close to the original CAD entity model based on the minimizing geometric criterion. It is generally used in computer numerical control (CNC) machining and rapid prototyping to represent the meshed surfaces [16]. With the specific chord error during discretization, the STL file uses a high density of triangular meshes to express the surface part where the curvature changes greatly. If the surface is flat, the triangular mesh density is sparse.

The data redundancy of STL file is large because there are lots of triangular meshes saved in the file, each of which includes three-dimensional coordinates of three vertices and the normal vector of the triangle. However, it does not contain the topology among triangular meshes. The path planning computation based directly on the STL file is very large. So, it is necessary to establish the topology of the STL format file.

The half-edge data structure is used to represent the topology of the model. In the structure, each edge of the triangle is split into two half-edges with opposite directions, and in one triangular the directions of all half-edges conform to the right hand rule. This structure is suitable for various geometric operations, such as finding neighbour information of vertices and triangles fast, traversing through all the vertices, edges and triangles without duplication.

The diagram of topology after the reconstruction is depicted in Fig. 3. Given a facet F_1, it is easy to find the vertices (P_1, P_2, P_3) of the facet and its three half-edges (E_1, E_2, E_3). Through the adjacent edge of one half-edge, the adjacent facet can be easily found. As in Fig. 3, E_4 which belongs to facet F_2 is the adjacent edge of the half-edge E_3 in facet F_1, so F_2 is one of the adjacent facets of F_1. When the edge is at the boundary of the model, the index of the half-edge is set to be 0. During the computing process, if the index of the adjacent edge of a half-edge is equal to 0, it means that the computation reaches the model boundary.

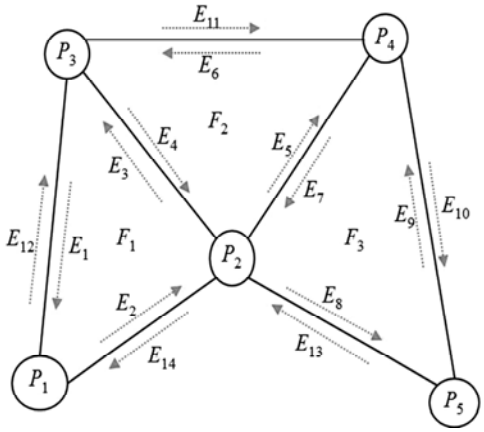

Figure 3. The diagram of STL topology reconstruction.

3.2 Definitions

3.2.1 Geodesic Offset

Geodesic offset of a curve on a surface can be depicted as a sequence of points, which are at a certain geodesic distance from the given curve as shown in Fig. 4. Geodesic offset direction is taken as the orthogonal direction [7].

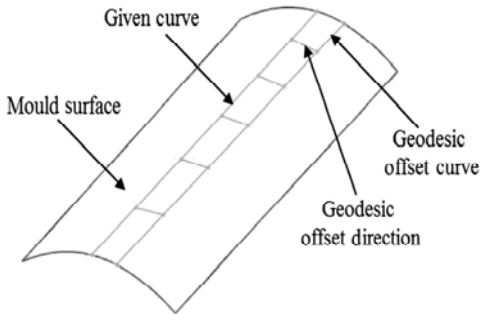

Figure 4. The diagram of geodesic offset.

3.2.2 Progenitor Curve and Descendant Curve

During the offsetting process, the curve on the surface which is taken as the reference to compute the next offset curve can be called the progenitor curve. The next curve obtained from the progenitor curve along the geodesic offset direction could be called the descendant curve. As in Fig. 4, the given curve can be taken as the progenitor curve, and the geodesic offset curve is the descendant curve.

3.2.3 Offset Point (OP) and General Point (GP)

On the meshed surface, the surface curve is constituted by a serial of line segments and each line segment between two consecutive points is in one triangular mesh. In order to reduce the calculation amount, the points which belong to surface curve are divided into two classes. One is called the OP where the geodesic offset direction needs to be computed; the other is called the GP and the offset direction is simple along edges starting from the point.

3.2.4 Offset Directional Segment (ODS)

ODS generally contains the start point which is on initial path, the end point, the offset direction and the offset angle which is between the offset direction and the line segment where the start point locates. For OP and GP on initial path, the ODSs are computed according to different rules.

The ODSs of GPs which locate at the vertex of the mesh or on the edge of the mesh are firstly decided. As shown in Fig. 5, the offset direction of the path at point P_1 is defined as below:

$$\boldsymbol{p} = \boldsymbol{n} \times \boldsymbol{P_1P_2} \tag{1}$$

where $\boldsymbol{p}$ represents the offset direction, $\boldsymbol{n}$ is the normal vector of the meshed surface where point P_1 locates, and $\boldsymbol{P_1P_2}$ states the direction of the path at point P_1.

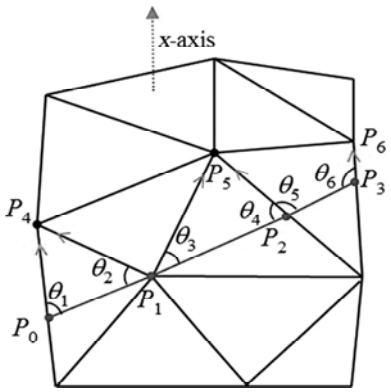

Figure 5. The generation of offset directional segments for GPs.

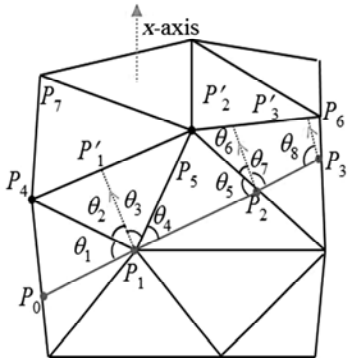

Figure 6. The generation of offset directional segments for OPs.

The ODSs are determined by two cases. One case is that points locate on the edge of the triangular mesh, such as P_0, P_2 and P_3, and the ODSs are the edges (P_0P_4, P_2P_5 and P_3P_6) with the start points mentioned above. These edges meet $\boldsymbol{P_0P_4} \cdot \boldsymbol{p} > 0, \boldsymbol{P_2P_5} \cdot \boldsymbol{p} > 0$ and $\boldsymbol{P_3P_6} \cdot \boldsymbol{p} > 0$. The end points of the ODSs are P_4, P_5 and P_6. The direction is from the start point to the end point, and the offset angles are θ_1, θ_4 and θ_6. When the start point as point P_2 does not locate at the surface boundary, the offset angle could choose θ_4 or θ_5 (often choosing the smaller). The other case is as point P_1 which is at the vertex of the triangular mesh. The ODSs are P_1P_4 and P_1P_5 with the common start point P_1. The directions also meet $\boldsymbol{P_1P_4} \cdot \boldsymbol{p} > 0$ and $\boldsymbol{P_1P_5} \cdot \boldsymbol{p} > 0$, and the offset angles are θ_2 and θ_3 correspondingly.

The computation to get the ODSs of OPs is depicted in Fig. 6. Assuming points P_0, P_1, P_2 and P_3 are OPs, their ODSs are constituted by two types. One type is the same as ODS of GP, which includes the edges such as edges P_1P_4 and P_1P_5 as for point P_1. The other type of ODS is the angular bisector and could be called the extra ODS. Because the curves on the meshed surface are compound curves, the exact perpendicular direction may not exist at some location of tangential discontinuity. So the angular bisector is chosen as the extra ODS for the OP on the initial path. As in Fig. 6, for P_1, the $P_1P'_1$ is an extra ODS with the condition ($\theta_1 + \theta_2 = \theta_3 + \theta_4$). Besides the vector $\boldsymbol{P_2P_5}$, $\boldsymbol{P_2P'_2}$ is the ODS of P_2 based on the situation ($\theta_5 + \theta_6 = \theta_7$). When the points locate at the surface boundary like P_0 and P_3, the angles between the edges and the directions of the initial path at that point are firstly computed. If the angle is less than 90°, the extra ODS for OP does not exist as P_0. Otherwise, the extra ODS for P_3 is $P_3P'_3$ with the offset angle being equal to 90°.

4. The Accurate Path Planning Algorithm in Robotic Fibre Placement

Generally, fibre tows are continually placed in one ply by the roller of the placement head at constant angles including 0°, 45°, −45° and 90°. The 0°, ±45°, 90° paths are often used to carry axial, shear and radial stresses. If the composite structure is under complex load, the plies of the structure are placed multidirectional according to the four angle types [17]. In RFP, the initial paths with angles 0°, 45°, −45° and 90° are firstly needed to be computed, the next paths are achieved by offsetting orthogonally from the initial paths.

4.1 Generation of the Initial Paths

The algorithm to generate initial paths refers to the section contour in the process of slicing algorithm, which is often used in the rapid prototyping technology [18]. During RFP process, the laying angle is often set by the reference line. For instance, the path is called 0° path when it is paralleled to the reference line. The path is called 90° when it is orthogonal to the reference line. So the initial reference lines should be firstly constructed, then the initial paths of different laying angles are produced on the basis of the reference line.

Taking the generation of 45° initial paths *e.g*, the slicing direction is taken as the reference line. The direction of initial 45° path is got by rotating the reference line anticlockwise along the normal vector of the meshed surface at the path point, as shown in Fig. 7. The point P_0 belongs to the half-edge E_1. Assuming that P_0 is the start point of 45° path which locates at the boundary of the meshed surface, the next path point P_1 could be obtained from P_0. In mesh F_1, the point P'_0 could be computed on the basis of the slicing algorithm, and the normal vector $\boldsymbol{n_{p0}}$ of the surface where point P_0 locates is set to be equal to normal vector of the mesh F_1. Taking the vector $\boldsymbol{P_0P_0'}$ as vector $\boldsymbol{t_1}$ to represent the reference line, rotating $\boldsymbol{t_1}$ with the

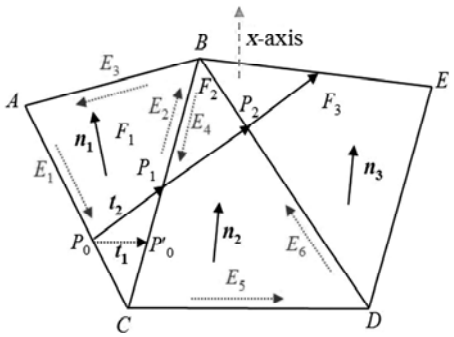

Figure 7. The diagram of path generation with 45°.

angle of 45° anticlockwise along $\boldsymbol{n_{p0}}$ to get the vector $\boldsymbol{t_2}$ just as (2), the intersection point P_1 between $\boldsymbol{t_2}$ and one of the other two half-edges (E_2 and E_3) of triangular mesh F_1 could be found through three-dimensional computational geometry.

$$\boldsymbol{t_2} = Rot(\boldsymbol{f}, \alpha) \cdot t_1 \tag{2}$$

Where

$$Rot(f,\alpha) = \begin{bmatrix} f_x f_x \mathrm{vers}\alpha + \cos\alpha & f_y f_x \mathrm{vers}\alpha - f_z \sin\alpha & f_z f_x \mathrm{vers}\alpha + f_y \sin\alpha \\ f_x f_y \mathrm{vers}\alpha + f_z \sin\alpha & f_y f_y \mathrm{vers}\alpha + \cos\alpha & f_z f_y \mathrm{vers}\alpha - f_x \sin\alpha \\ f_x f_z \mathrm{vers}\alpha - f_y \sin\alpha & f_y f_z \mathrm{vers}\alpha + f_x \sin\alpha & f_z f_z \mathrm{vers}\alpha + \cos\alpha \end{bmatrix} \tag{3}$$

$\boldsymbol{f} = [f_x, f_y, f_z]$ is the general rotation normal vector, f_x, f_y, f_z are the components of $\boldsymbol{f}$, and $\boldsymbol{f} = \boldsymbol{n_{p0}}, \alpha = 45°$, $\mathrm{vers}\,\alpha = 1 - \cos\alpha$.

Vector $\boldsymbol{t_2}$ shows the direction of 45° path and other points of 45° paths are computed in this direction. The computation from P_1 to get P_2 is illustrated as below. The normal vector of surface at point P_1 and the vector $\boldsymbol{t_2}$ constitute a plane v. The binormal vector $\boldsymbol{k}$ of the meshed surface where point P_1 locates is established as follow:

$$\boldsymbol{k} = \boldsymbol{n_{p1}} \times \boldsymbol{t_2} = [x_k,\ y_k,\ z_k]^T \tag{4}$$

So the equation of plane v with the point $P_1(x_1, y_1, z_1)$ is showed as below:

$$x_k(x - x_1) + y_k(y - y_1) + z_k(z - z_1) = 0 \tag{5}$$

The intersection line between the plane v and mesh F_2 is the line segment of the 45° path, and the end point P_2 is the required path point. Other path points could be computed by such method until the calculation reaches the surface boundary.

The normal vector of the meshed surface at a point is defined as in Fig. 8. If the point lies inside a facet as P_1, the normal vector of the facet is taken as the normal vector of the surface at that point, *i.e.* $\boldsymbol{n_{p1}} = \boldsymbol{n_1}$. If the point locates on an edge as point P_3, the average normal vector of the adjacent facets is taken as the normal vector of the surface at point P_3, *i.e.* $\boldsymbol{n_{p3}} = 1/2 * (\boldsymbol{n_4} + \boldsymbol{n_7})$. When the point is at the vertex of the triangular mesh as P_2, the average normal vector of all the facets converged at point P_2 is taken as the normal vector of the surface at the point, *i.e.* $\boldsymbol{n_{p2}} = 1/6 * (\boldsymbol{n_1} + \boldsymbol{n_2} + \boldsymbol{n_3} + \boldsymbol{n_4} + \boldsymbol{n_5} + \boldsymbol{n_6})$.

Initial paths of angle 0°, 45°, −45°, 90° are produced using the proposed method as shown in Fig. 7. They are the straightest lines at each laying angle direction, taking into account the variation of normal vector of meshed surface along the path [19].

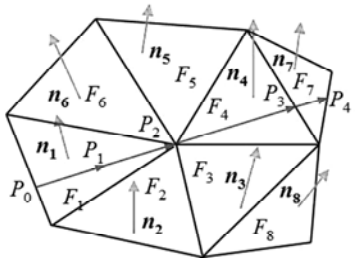

Figure 8. The diagram of surface normal at some point.

4.2 Offset Paths Construction

A basic requirement of paths in RFP is that there are minimal gaps and overlaps between two courses. So the number of fibre tows in one course is constant as much as possible during the laying process, which will also improve the efficiency of the fibre laying and reduce the times of cutting and restarting of fibre tows. When obtaining the offset paths from the initial paths, the incremental approach [14] is adopted to produce the intermediate offset curves. The method to produce the offset direction is introduced, and the requirement of the placement error is considered in the paper to guarantee the fibre tows to be placed completely on the mould surface.

The initial paths obtained above are a set of line segments and all points on initial paths are chosen to be offset along the ODSs. So offset distances along the ODSs and the extra ODSs together determine the descendant curve as in Fig. 9. The solid line segments on the descendant path are totally computed by the extra ODS, but the dotted line segments are got with the help of ODSs. The two kinds of line segments ensure that each line segment of the path between two consecutive points lies exactly on one triangular mesh.

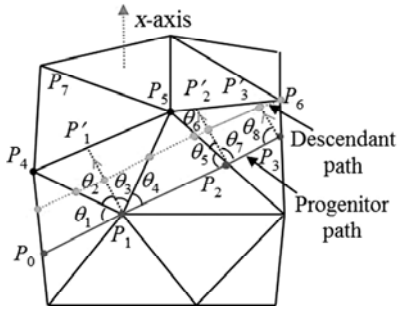

Figure 9. The diagram of offset line segments.

4.2.1 Computation of the Offset Distance

In RFP, the actual width of fibre tows placed on the surface is computed along the perpendicular direction as shown in Fig. 10. Supposing ODS of P_2 is P_2P_3 with the angle being θ, the offset direction is along the x axis. If $|P_2P_3| = d$, where $||$ represents the length of the line segment, points P_1 and P_2 locate on the initial path, $\boldsymbol{P_3P'_3}$ is perpendicular to the vector $\boldsymbol{P_1P_2}$. If $|\boldsymbol{P_3P'_3}| = d_n$, the relationship between d and d_n is established as below:

$$d_n = d * \sin(\theta) \tag{6}$$

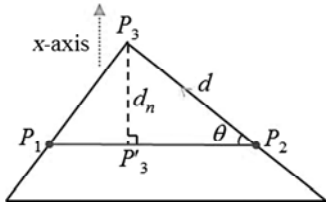

Figure 10. The relationship between d and d_n.

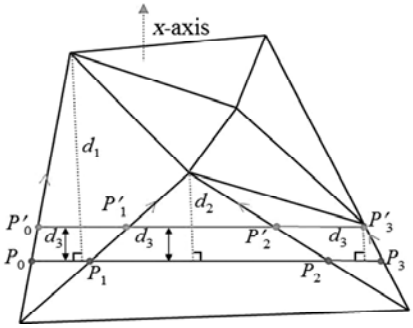

Figure 11. The diagram of curve offsetting.

Seen from Fig. 11, along the perpendicular direction in the mesh, the distances that each line segment can offset are d_1, d_2, d_3, and the minimal distance $d_{\min}$ is found, here $d_{\min} = d_3$. Assuming the given offset distance is D_{offset}, if $d_{\min} = D_{\text{offset}}$, the final offset curve which is constituted by line segments ($P'_0P'_1$, $P'_1P'_2$ and $P'_2P'_3$) is obtained. If $d_{\min} > D_{\text{offset}}$, the final offset can be got by computing once. Otherwise, $D_{\text{offset}} = D_{\text{offset}} - d_{\min}$, and the offset process is executed to get the final offset curve. In such case, the already achieved offset curve could be called the intermediate offset curve which is also set as the progenitor curve to get the descendant curve. For the points on the intermediate curve, if they reach the end point of the corresponding ODSs, the new ODSs need to be computed. Otherwise, the points could offset along the current ODSs.

4.2.2 Determination of the Number of Fibre Tows

During offsetting process, the length sum L of all the d_n in Fig. 10 represents the width of the offset distance in one placement. The sum L is no more than the maximal width D, *i.e.* $L \le D, D = d \times N_{num}$, and d is the width of one fibre tow, and N_{num} is the maximal number of fibre tows in one course. At the same time, the offset distance also needs to meet the requirement of placement error Δ [8].

All the points on a serial of extra ODSs constitute the trajectory of the roller which is mounted on the placement head. The distribution of these points on meshed surface could be classified into three categories as shown in Fig. 12.

For every offset point on initial paths, the maximal width D and the offset distance of meeting the placement error Δ are often different. For each OP on initial paths, its corresponding offset distance is firstly accomplished with the sum length (being equal to D) of the extra ODS sequence. Then the maximal allowable offset

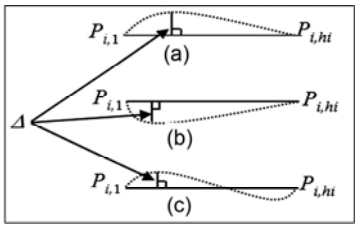

Figure 12. The diagram of placement error Δ.

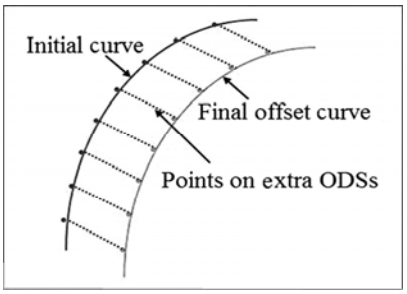

Figure 13. The diagram of offset curve.

distance could be achieved, meeting the placement error requirement $\Delta_i < \Delta_{\max}$ by the following steps:

Step 1. According to offset direction, suppose point $P_1 = P_{i,1} (i = 1, 2, \ldots, n,$ where n is the number of offset points) as the start point which is on the initial path, and take point $P_2 = P_{i,hi}$ as the end point, where h_i is total number of points which constitute the serial of extra ODSs of $P_{i,1}$, and connect the two consecutive points to constitute the line segment l_i.

Step 2. Compute the projection distances of every point between the start and the end point to the line l_i. Then find the maximal distance $d_{\max}$.

Step 3. If $d_{\max} \le \Delta_{\max}$, the maximal allowable offset distance L_i from $P_{i,1}$ to $P_{i,hi}$ is saved. Otherwise set $h_i = h_i - 1$, return to step 2.

Step 4. Compare all the length $L_i (i = 1, 2, \ldots, n)$, find the minimal length $L_{\min}$. Then let $D_{\text{offset}} = L_{\min}$, compute $N = [D_{\text{offset}}/d]$, where d is the width of one fibre tow, and D_{offset} is the offset distance, [ ] is the round operator. Then let $D_{\text{offset}} = N * d$.

Step 5. For every offset point P_i on initial path, compute the length of line segments along the extra ODS direction. When the length is equal to D_{offset}, the final offset point is saved. After all the offset points are acquired, the final offset curve is achieved by fitting a curve to this set of final offset points, as shown in Fig. 13.

From the above steps, the offset curve of the initial path is obtained. Taking the offset curve as the initial curve, the next offset curve could be achieved from the above steps in this part.

5. Simulation Results of the Proposed Algorithm

5.1 Simulation

The freeform surface model as in Fig. 14 is taken as the meshed surface with the chord error 0.3 mm to validate

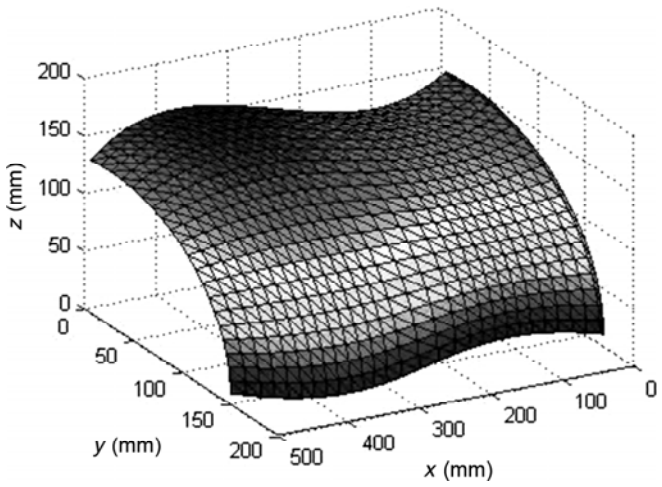

Figure 14. Triangular meshes of the freeform surface model.

the proposed algorithm. The initial paths of 0°, 90° and ±45° are obtained in Fig. 15. The OPs and GPs are chosen alternatively from the points which are connected to constitute the initial paths. The rest paths are generated along the perpendicular directions of the initial paths on the meshed surface. The offset distances are no more than the maximal width of one course and also meet the placement error ($\Delta \leq 2.0\,\text{mm}$) which could ensure the fibre tows to be placed on the mould surface completely. All paths achieved are shown in Fig. 16. The number of fibre tows in each course is listed in the following tables in detail.

From Table 1–4, with the width of each fibre tow 3.2 mm, the offset distances at different parts of the surface, meeting the placement error, are different. Most of the number of fibre tows in one course is less than the maximal number. Although the placement efficiency will reduce, all the fibre tows could be pressed by the roller on the surface completely which could guarantee the placement effect.

5.2 Analysis of the Proposed Method

With the initial paths being the straightest lines on the meshed surface along the given direction, the angular bisector is chosen as the geodesic offset direction which represents the roller location during the placement. The angle θ between the extra ODS and the corresponding line segment where the start point locates is almost equal to 90°. Sin(θ) is almost the same as the value of sin(90°) and the maximal error between the two values for all the serial of extra ODSs during the computation is less than 1e–5, so the angular bisector of the initial path is taken as the offset direction is reasonable.

5.2.1 Compared with the Algorithm in [15]

The path planning method introduced in [15] can generate four laying angles, but the number of fibre tows in one course is variable which needs the placement head to restart or cut the fibre tow during the process. Figure 17 depicts the paths generated by the method in [15] with the laying angle being 90°. During placement along one path, the number of fibre tows is variable as in Fig. 18. The

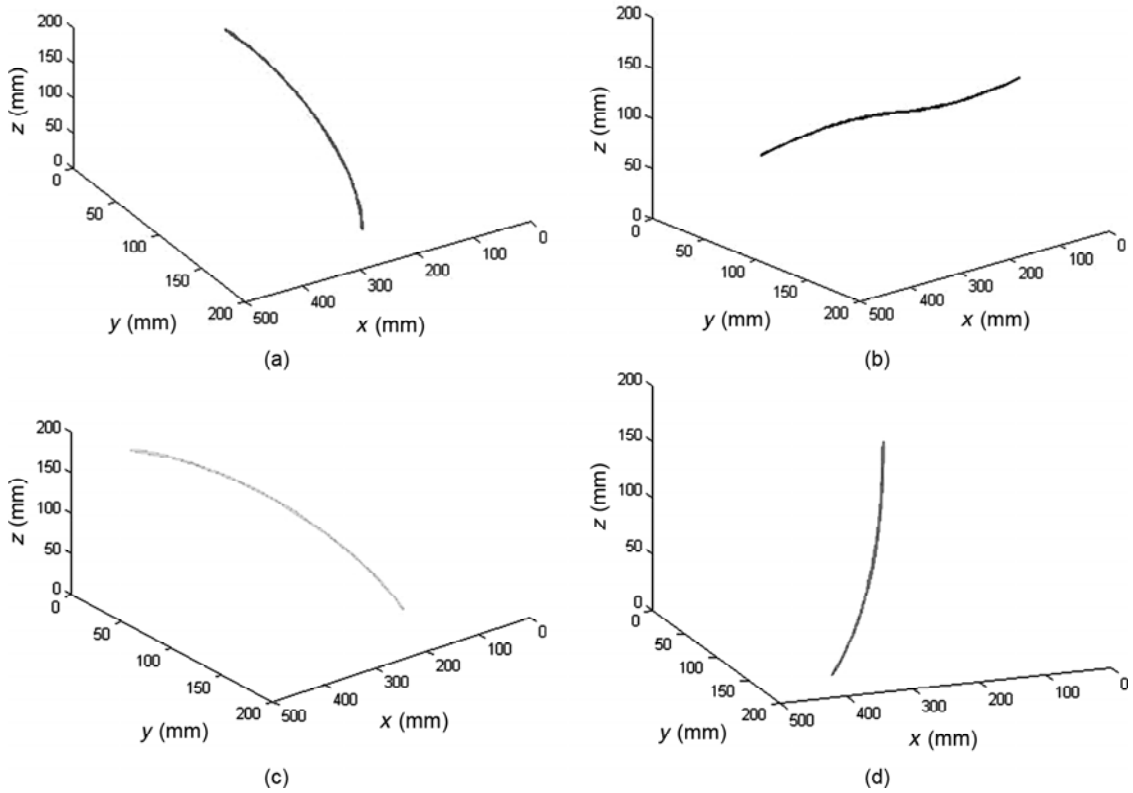

Figure 15. The initial paths with different angles: (a) 0°; (b) 90°; (c) 45°; and (d) –45°.

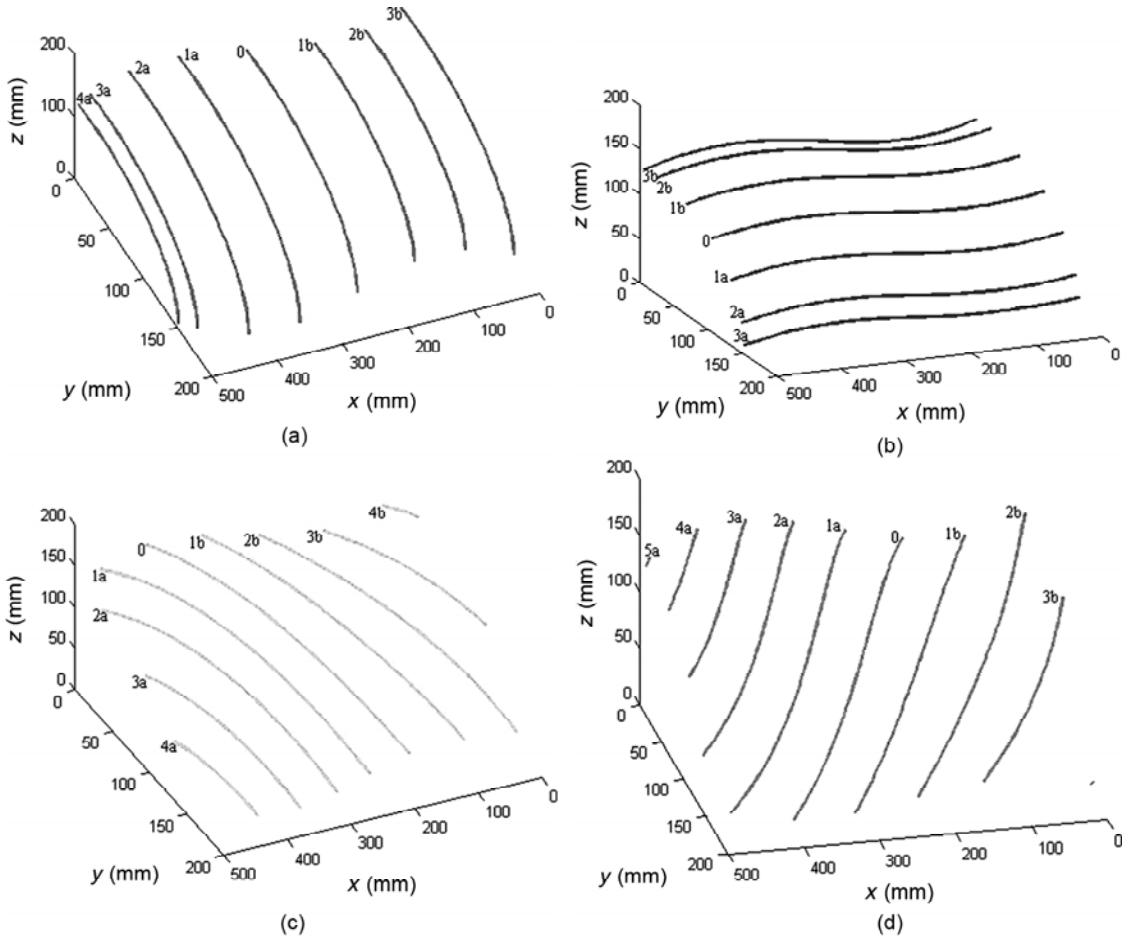

Figure 16. The generated paths with different angles: (a) 0°; (b) 90°; (c) 45°; and (d) −45°.

Table 1
The Number of Fibre Tows with Angle 0°

No.	0–1a	1–2a	2–3a	3–4a	0–1b	1–2b	2–3b
Fibre tows num	32	24	20	7	32	24	19
Offset dist (mm)	102.4	76.8	64	22.4	102.4	76.8	60.8

Table 2
The Number of Fibre Tows with Angle 90°

No.	0–1a	1–2a	2-3a	0–1b	1–2b	2–3b
Fibre tows num	13	13	6	13	13	7
Offset dist (mm)	41.6	41.6	19.2	41.6	41.6	22.4

number $1, 2, 3, \ldots$, and 15 are points where the placement head needs to cut or restart fibre tows. The number $29, 28, 27, \ldots$, and 27 are corresponding quantity of the fibre tows in one course at different locations.

However, as in Fig. 16(b), the number of fibre tows in one course is constant. On one hand this can reduce the

Table 3
The Number of Fibre Tows with Angle 45°

No.	0–1a	1–2a	2–3a	3–4a	0–1b	1–2b	2–3b	3–4b
Fibre tows num	17	15	16	15	19	18	19	20
Offset dist (mm)	54.4	48	51.2	48	60.8	57.6	60.8	64

Table 4
The Number of Fibre Tows with Angle −45°

No.	0–1a	1–2a	2–3a	3–4a	4–5a	0–1b	1–2b	2–3b	3–4b
Fibre tows num	17	16	15	15	14	18	19	18	28
Offset dist (mm)	54.4	51.2	48	48	44.8	57.6	60.8	57.6	89.6

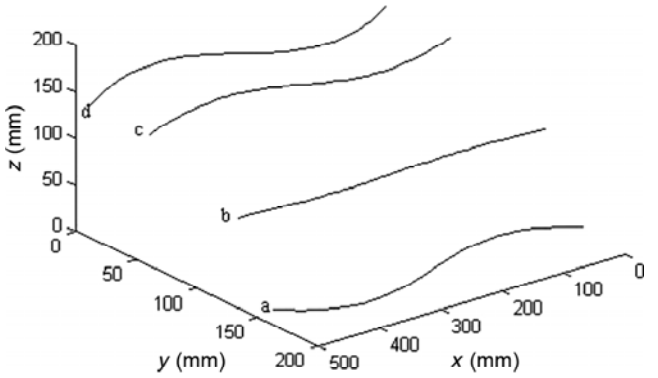

Figure 17. The generated paths with angle 90° using the method in [15].

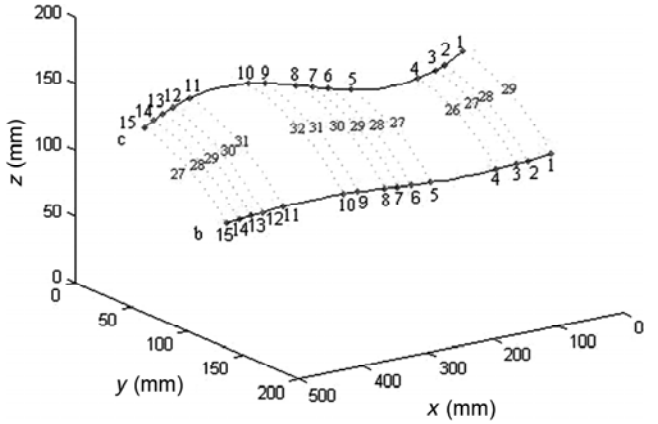

Figure 18. The variable number of fibre tows in one course during placement.

times of cutting and restarting motion conducted by the placement head to improve the laying efficiency and also avoid gaps and overlaps because of cutting and restarting fibre tows during placing. On the other hand, the invariable number of fibre tows meets the placement error requirement which ensures fibre tows to be pressed on the mould surface completely.

5.2.2 Compared with the Constant Offset Distance Algorithm

The method in this paper compares with the constant offset distance which does not consider the placement error in [7]. Taking the first offset distance with four commonly used angles in one side *e.g.*, the placement errors produced by two methods are compared in Fig. 19. The number 32 is the maximal number of fibre tows in one course and the number N are 32, 13, 17, and 17 separately. The width of each fibre tow is 3.2 mm. The dotted curve represents the placement error of the proposed algorithm in the work. The dot-dash line expresses the placement error with placing the maximal number of fibre tows in one course.

In Fig. 19(a), the placement errors produced by two methods are the same. In Fig. 19(b), (c) and (d), the number N is less than 32 ensuring the placement error is less than 2.0 mm which is set to be the maximal placement error. When fibre tows with maximal number in one course are placed in [7], the error of placement often exceeds the error threshold. Meanwhile, the other courses produced by the presented algorithm are all under the placement error.

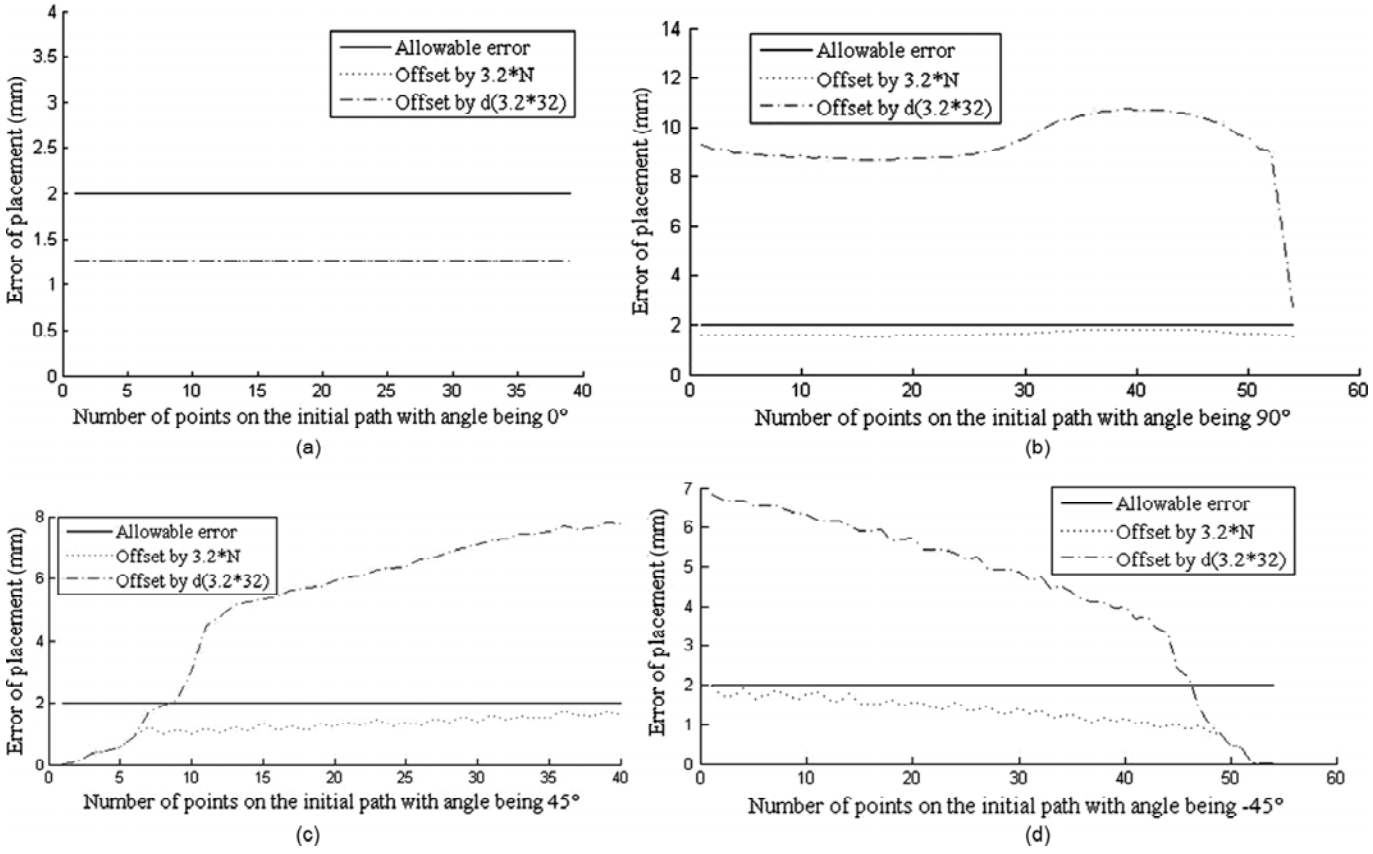

Figure 19. Comparisons of placement errors with different angles: (a) 0°; (b) 90°; (c) 45°; and (d) −45°.

6. Conclusion

In this paper, an accurate path planning algorithm for RFP based on triangular meshes is produced. Firstly, initial paths of commonly used angles are produced, and other paths are then generated by offsetting a distance along the certain direction with meeting the placement error. The algorithm has the advantage of working on a triangular mesh for describing the surface rather than on its parametric equation. This feature makes it easy to obtain the placement trajectories for structures with complex geometry. Moreover, it computes the fibre laying paths with meeting the placement error which makes the fibre tows placed on the surface completely, and the constant number in one course makes it avoid the gaps and overlaps which could improve the forming precision of composite structures.

In the future work, there is a need to optimize the step of choosing the OPs on the initial path. It is worth establishing an equation to express the relationship between the surface curvature and the choosing OPs step which ensures the ODS sequences cover all surface features. Meanwhile, the quantity of OPs is as little as possible to reduce the amount of computation.

Acknowledgement

This work is partly supported by The National Natural Science Foundation of China (Grant No. 61421004) and The National Natural Science Foundation of China (Grant No. 51405486).

References

[1] G. Marsh, Automating aerospace composites production with fibre placement, *Reinforced Plastics*, *55*(3), 2011, 32–37.

[2] P. Debout, H. Chanal, and E. Duc, Tool path smoothing of a redundant machine: Application to automated fiber placement, *Computer-Aided Design*, *43*(2), 2011, 122–132.

[3] T. Aized and B. Shirinzadeh, Robotic fiber placement process analysis and optimization using response surface method. *The International Journal of Advanced Manufacturing Technology*, *55*(1–4), 2011, 393–404.

[4] B. Shirinzadeh, G. Alici, C.W. Foong, and G. Cassidy, Fabrication process of open surfaces by robotic fibre placement, *Robotics and Computer-Integrated Manufacturing*, *20*(1), 2004, 17–28.

[5] A. Kumar and A. Ojha, Subdivision-based corridor map method for path planning, *International Journal of Robotics and Automation*, *28*(4), 2013, 331–339.

[6] A.H.A. Hafez, A.K. Nelakanti, and C.V. Jawahar, Path planning for visual servoing and navigation using convex optimization, *International Journal of Robotics and Automation*, *30*(3), 2015, 299–307.

[7] B. Shirinzadeh, G. Cassidy, D. Oetomo, G. Alici, *et al.*, Trajectory generation for open-contoured structures in robotic fibre placement, *Robotics and Computer-Integrated Manufacturing*, *23*(4), 2007, 380–394.

[8] L. Yan, Z.C. Chen, Y. Shi, and R. Mo, An accurate approach to roller path generation for robotic fibre placement of free-form surface composites, *Robotics and Computer-Integrated Manufacturing*, *30*(3), 2014, 277–286.

[9] W. Zeng, J. Xiao, Y. Li, D.J. Huan, *et al.*, Research on path planning and coverability analysis of automatic fiber placement for structures in revolving shell, *Journal of Astronautics*, *31*(1), 2010, 239–243.

[10] X.D. Dang, J. Xiao, and D.J. Huan, Implementation on fiber placement parallel equidistant path generation algorithm, *Journal of Wuhan University* (*Natural Science Edition*), *53*(5), 2007, 613–616.

[11] H.Y. Lin, C.Y. Ho, and M.L. Wang, Reverse engineering of geometric models using images of surface level curves, *International Journal of Robotics and Automation*, *24*(2), 2009, 115–124.

[12] J.T. Xu, W.J. Liu, H.Y. Bian, and H.B. Wang, Constant scallop tool path for triangular surface machining, *Journal of Mechanical Engineering*, *46*(11), 2010, 193–198.

[13] W.L. Xiong, J. Xiao, X.F. Wang, J.X. Li, *et al.*, Algorithm of adaptive path planning for automated placement on meshed surface, *Acta Aeronautica ET Astronautica Sinica*, *34*(2), 2013, 434–441.

[14] V.D. Holla, K.G. Shastry, and B.G. Prakash, Offset of curves on tessellated surfaces, *Computer-Aided Design*, *35*(12), 2003, 1099–1108.

[15] L.N. Li, X.G. Wang, D. Xu, and M. Tan, A placement path planning algorithm based on meshed triangles for carbon fiber reinforce composite component with revolved shape, *IJCS: International Journal on Control Systems and Applications*, *1*(1), 2014, 23–32.

[16] Y.W. Sun, J. Liu, and W.J. Liu, Reconstructing accurate boundary representation from STL model, *Journal of Computer-Aided Design & Computer Graphics*, *16*(7), 2004, 944–949.

[17] L.L. An, Y. Zhou, and L.S. Zhou, Composite fiber placement path planning and fiber number determination, *Acta Aeronautica ET Astronautica Sinica*, *28*(3), 2007, 745–750.

[18] G. Yang, W.J. Liu, W. Wang, and L.Y. Qin, Research on the rapid slicing algorithm based on STL topology construction, *Advanced Materials Research*, *97–101*, 2010, 3397–3402.

[19] G.V.V.R. Kumar, P. Srinivasan, V.D. Holla, K.G. Shastry, *et al.*, Geodesic curve computation on surfaces, *Computer Aided Geometric Design*, *20*(2), 2003, 119–133.

Biographies

Lina Li received her B.Sc. degree from Taiyuan University of Technology, Taiyuan, China, in 2008, and her M.Sc. degree from Beijing Institute of Technology, Beijing, China, in 2010. Currently, she is a Ph.D. candidate in the Institute of Automation, Chinese Academy of Sciences (IACAS), Beijing, China. Her research interests include robotic control and path planning.

Xingang Wang received his B.Sc. degree from Tianjin University, Tianjin, China, in 1995 and his Ph.D. degree from Changchun Institute of Optics, Fine Mechanics and Physics, Chinese Academy of Sciences, Changchun, China, in 2002. He is currently a professor in the Research Center of Precision Sensing and Control, Institute of Automation, Chinese Academy of Sciences. His research interests include image processing and machine learning.

De Xu received his B.Sc. and M.Sc. degrees from Shandong University of Technology, Jinan, China, in 1985 and 1990, respectively, and his Ph.D. degree from Zhejiang University, Hangzhou, China, in 2001, all in control science and engineering. Since 2001, he has been with the Institute of Automation, Chinese Academy of Sciences (IACAS), Beijing, China, where he is currently a professor in the Research Center of Precision Sensing and Control. His research interests include robotics and automation, in particular, the control of robots, such as visual control and intelligent control.

Min Tan received his B.Sc. degree from Tsing Hua University, Beijing, China, in 1986, and his Ph.D. degree from the Institute of Automation, Chinese Academy of Sciences (IACAS), Beijing, China, in 1990, both in control science and engineering. He has been with IACAS since 1990. He is currently a professor with the State Key Laboratory of Management and Control for Complex Systems, IACAS. He has published over 100 papers in journals, books and conferences. His current research interests include robotics, robot vision and intelligent control systems.